Grayscale Femtosecond Laser Directly Writing of Apodized Chirped Fiber Bragg Gratings With Pulse Timing Control

Zesen Zhang, Yiping Wang , Senior Member, IEEE, Fellow, Optica, Dejun Liu, Jiajun Guan, Shangben Jiang, Kaiming Yang, Ying Wang, Jun He, Member, IEEE, and Changrui Liao

Abstract—Chirped fiber Bragg gratings (CFBGs) are widely applied in telecommunications, sensing, and ultrafast laser systems due to their broadband dispersion properties. However, fabrication of CFBGs with a linear group delay remains a challenge. This study introduces a novel fabrication technique that integrates femtosecond grayscale lithography with external pulse timing control to produce CFBGs with high coupling efficiency, precise dispersion compensation, and well-controlled linear chirp rates. CFBGs with varying dispersion profiles were fabricated, achieving dispersion errors below 0.2 ps/nm. To further enhance the spectral performance, three apodization functions (Hamming, Triangular, and Gaussian) were applied to CFBGs. Both simulations and experiments demonstrate that these apodization functions effectively suppress reflection spectra side lobes and improve group delay linearity. Notably, the Gaussian apodization function yields superior results, achieving a side-lobe suppression ratio (SLSR) exceeding 15 dB and optimal spectral performance. The proposed fabrication method of CFBGs provides new possibilities for telecommunications, high power laser system and other cutting-edge scientific research.

Received 24 April 2025; revised 16 June 2025 and 24 June 2025; accepted 25 June 2025. Date of publication 7 July 2025; date of current version 2 September 2025. This work was supported in part by the National Key Research and Development Program of China under Grant 2024YFB3213700, in part by the National Natural Science Foundation of China under Grant 62475170, Grant 62475161, and Grant U22A2088, in part by Guangdong Basic and Applied Basic Research Foundation under Grant 2023A1515012893 and Grant 2022B1515120061, in part by the Shenzhen Science and Technology Program under Grant JCYJ20220818095800001 and Grant JCYJ20220818095615034, in part by the Shenzhen Key Laboratory of Ultrafast Laser Micro/Nano Manufacturing under Grant ZDSYS20220606100405013, in part by the Research Team Cultivation Program of Shenzhen University under Grant 2023QNT009, in part by the Medicine Plus Program of Shenzhen University under Grant 2024YG013, and in part by the Scientific Foundation for Youth Scholars of Shenzhen University under Grant 806-0000340601. (Zesen Zhang and Yiping Wang contributed equally to this work.) (Corresponding author: Dejun Liu.)

Zesen Zhang, Yiping Wang, Dejun Liu, Jiajun Guan, Shangben Jiang, Ying Wang, Jun He, and Changrui Liao are with the Shenzhen Key Laboratory of Ultrafast Laser Micro/Nano Manufacturing, Key Laboratory of Optoelectronic Devices and Systems of Ministry of Education and Guangdong Province, College of Physics and Optoelectronic Engineering, Shenzhen University, Shenzhen 518060, China, and also with the Guangdong and Hong Kong Joint Research Centre for Optical Fiber Sensors, Shenzhen University, Shenzhen 518060, China (e-mail: 2300453049@email.szu.edu.cn; ypwang@szu.edu.cn; anmeliu@163.com; 2210452029@email.szu.edu.cn; 2450233005@mails.szu.edu.cn; yingwang@szu.edu.cn; hejun07@szu.edu.cn; cliao@szu.edu.cn).

Kaiming Yang is with the Shenzhen Institute of Information Technology, Shenzhen 518172, China (e-mail: yangkm@sziit.edu.cn).

Color versions of one or more figures in this article are available at https://doi.org/10.1109/JLT.2025.3585535.

Digital Object Identifier 10.1109/JLT.2025.3585535

Index Terms—Apodized grating, chirped grating, femtosecond laser directly writing, fiber Bragg grating.

I. INTRODUCTION

► HIRPED fiber Bragg gratings (CFBGs) have demonstrated remarkable versatility across telecommunications, sensing, quantum photonics, and ultrafast laser systems due to their broadband dispersion properties. In fiber-optic communications, CFBGs enable dispersion compensation and pulse compression, enhancing signal integrity and data rates by counteracting pulse broadening [1], [2], [3]. CFBGs can be also used for sensing applications, such as monitoring of strain [4], temperature [5], materials [6], and pressure [7], [8]. In quantum photonics, CFBGs offer tailored dispersion for efficient singlephoton generation—for instance, Remesh et al. [9] demonstrated a compact, fiber-integrated CFBG system enabling robust adiabatic rapid passage excitation of quantum dots, paving the way for scalable quantum technologies. Additionally, CFBGs are pivotal in chirped-pulse amplification (CPA) systems, where their compact size and precise dispersion control facilitate highpower, ultrashort pulse generation. Examples include Bartulevicius et al. [10], who achieved 26 MW peak power with 349 fs pulses using CFBG stretchers, and Li F et al. [11], who realized a hybrid fiber-crystal CPA system delivering 1.5 GW peak power at 358 fs with near-diffraction-limited beam quality $(M^2 < 1.3)$.

Currently, two main methods have been proposed for the fabrication of CFBGs: the phase mask method and the femtosecond laser direct writing technique. The phase mask method utilizes the interference of UV light with a customized phase mask to imprint the grating pattern into the fiber core. This approach offers excellent consistency, making it well-suited for large-scale production. However, this method requires the prior preparation of customized phase masks and specialized optical fibers, such as photosensitive fibers [12], highly rareearth-doped fibers [13] and hydrogen-carrying fibers [14]. Additionally CFBGs fabricated by this method can be easily erased under high temperature, so it can only be used for relatively low temperature applications (usually below 200°C) [15]. In contrast, the femtosecond direct writing technique employs ultrashort laser pulses to induce periodic refractive index modifications (RIM) in the fiber core through nonlinear absorption effects,

0733-8724 © 2025 IEEE. All rights reserved, including rights for text and data mining, and training of artificial intelligence and similar technologies. Personal use is permitted, but republication/redistribution requires IEEE permission. See https://www.ieee.org/publications/rights/index.html for more information.

hence they can work normally up to 1000 [16], and there is no need for specialized masks and photosensitive fibers. For example, Koptev M Y et al. [17] demonstrates the use of femtosecond laser-inscribed CFBGs in ytterbium-doped fibers to compensate for spectral losses and enable effective pulse stretching in a fiber CPA system, achieving near-original pulse compression.

While femtosecond laser direct writing offers rapid and flexible fabrication of CFBGs, several technical limitations persist. The most significant challenge arises from nonlinear absorption of laser energy introduced substantial insertion losses and side lobes in spectrum. Current approaches to mitigate these effects include beam shaping [18], [19] and apodization function techniques [20]. Applying apodization function is simpler than beam shaping, but existing methods are limited to diagonal grating writing paths, leading to reduced coupling efficiency from core misalignment. Furthermore, existing method for point-bypoint inscription of apodized chirped FBGs is realized using laser with constant pulse repetition rate, with varied grating period achieved by adjusting the translation platform's movement speed. The acceleration and deceleration of the translation platform will introduce errors in the grating period, leading to inaccuracies in chirp rates and dispersion [21]. Current displacement platforms lack the necessary accuracy to achieve this smooth chirp profile, forcing reliance on discrete period splicing to create step-chirped approximations [22]. However, these compromised implementations consistently fail to deliver satisfactory spectral flatness. Hence there is an urgent need for developing novel fabrication methodologies capable of producing high-quality linear CFBGs.

In this paper, we propose a novel method for fabrication of apodized CFBGs by integrating femtosecond grayscale lithography [23], [24], [25] and external pulse timing control technique [26], this method uses constant platform movement speed but varied delay between pulses, hence there is no need to account for platform acceleration and deceleration, ensuring more accurate and controlled grating fabrication. with high coupling efficiency, precise dispersion compensation, and well-controlled linear chirp rates. Leveraging this platform, we successfully produced various apodized FBGs and CFBGs with different chirp rates and dispersion profiles. Experimental results confirm that the apodized gratings achieves a high side-lobe suppression ratio (SLSR) exceeding 15 dB, while keeping the deviation between theoretical and experimental dispersion values below 0.2 ps/nm. This approach overcomes the limitations of conventional femtosecond direct-write fiber grating techniques, offering a promising pathway for designing high-performance CFBGs.

II. THEORETICAL MODEL

Based on the coupled-mode theory, the refractive index modulation of an apodized CFBG can be expressed as [27], [28]:

$$n(z) = n_{eff} \left[1 + f(z) \cdot \cos \left(\frac{2\pi}{\Lambda(z)} z + \varphi(z) \right) \right], 0 \le z \le L$$

$$\varphi(z) = F \frac{z^2}{L^2} \tag{2}$$

Where n(z) represents the refractive index of the fiber core at different position z along the fiber, \mathbf{n}_{eff} is the effective refractive index of the fiber, f(z) denotes the amplitude variation of the induced refractive index modulation (apodization function), $\Lambda(z)$ represents the fiber grating period function, L is the grating length and $\varphi(z)$ is the phase function, where F is the chirp rate.

The propagation differences of light with different frequencies in the fiber can be quantified by the time delay as:

$$\tau_g = \frac{2L}{v_g} = \frac{2n_{eff}L}{c} \tag{3}$$

Where τ_g represents the group delay (GD) generated when the optical signal passes through the fiber grating, v_g denotes the average group velocity of light through the fiber, and c is the speed of light in a vacuum.

Once the grating length L and the operating wavelength λ are determined, the chirp rate F can be calculated as follows [29]:

$$F = \frac{m\Delta\lambda}{2L} = \frac{m(\lambda(z) - \lambda(0))}{2L} = \frac{8\pi n^2(z)L^2}{\lambda^2 cDL_f}$$
(4)

where m represents the diffraction order of the grating, $\Delta\lambda$ denotes the full width at half maximum (FWHM) of CFBG, $\lambda(z)$ indicates the variation of wavelength with position $z; L_f$ is the total length of the fiber, and D is the group velocity dispersion (GVD), which describes the velocity delay between light of different frequencies per unit length.

Based on the theoretical model, key parameters of the CFBG—including chirp rate, bandwidth, and grating length—can be determined from the target dispersion value.

III. THEORETICAL SIMULATION

The apodization function of a grating is vital to shape the spectrum and suppression of side lobes. Before experimental investigation, the spectral performances of FBGs and CFBGs with different apodization functions are simulated based on a beam propagation method (BPM). In the simulation, the apodized FBG has an apodization cofficient of 5×10^{-6} , with a central wavelength of 1550 nm and a resonance attenuation of -0.165 dB. while the apodized CFBGs has a central wavelength of 1550 nm, a bandwidth of 20 nm, a chirp rate of 10 nm/cm, and a grating length of 535.5 μ m.

Fig. 1 presents the reflection and transmission spectra of FBGs before and after applying three different apodization functions of Hamming, Triangular and Gaussian. The simulated grating lengths are 267.75 μ m, 428.4 μ m, 535.5 μ m and 535.5 μ m, with corresponding SLSR of 6.533 dB, 11.439 dB, 11.409 dB and 13.139 dB, respectively. The results indicate that the Gaussian apodization function achieves the most effective side lobe suppression.

The effect of different apodization functions on the spectral characteristics of CFBGs is also investigated as shown in Fig. 2. The simulated resonance attenuations for CFBGs without

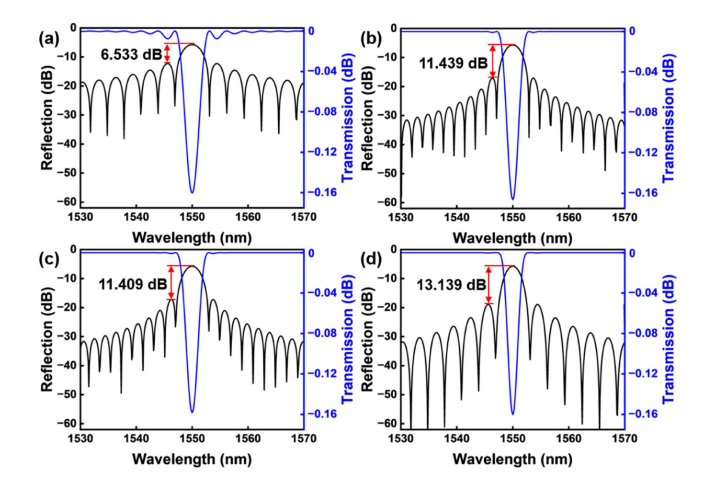


Fig. 1. Simulated reflection and transmission spectra of FBGs by different apodized functions: (a) non-apodized FBG with a grating length of 267.75 μ m and SLSR of 6.533 dB, (b) Hamming function of FBG with a grating length of 428.4 μ m and SLSR of 11.439 dB, (c) Triangular function of FBG with a grating length of 535.5 μ m and SLSR of 11.409 dB, and (d) Gaussian function of FBG with a grating length of 535.5 μ m and SLSR of 13.139 dB.

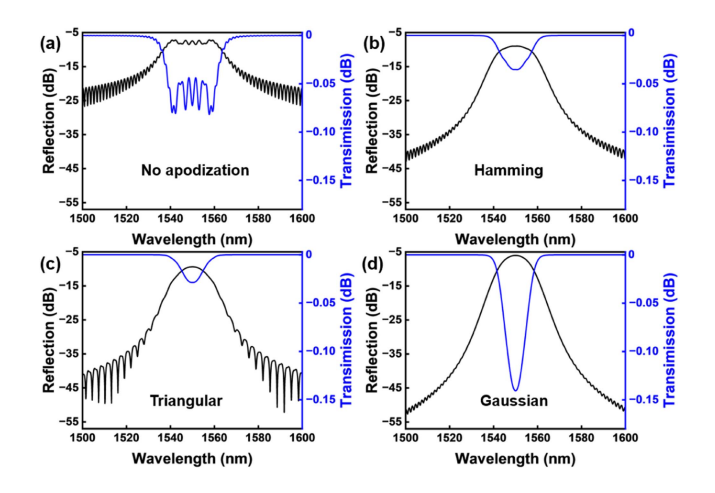


Fig. 2. Simulated reflection and transmission spectra of CFBGs with grating lengths of 535.5 μ m by different apodized functions: (a) non-apodized function, (b) Hamming function, (c) Triangular function, and (d) Gaussian function.

apodization functions and with Hamming, Triangular and Gaussian apodization functions are -0.07 dB, -0.03 dB, -0.03 dB and -0.14 dB, respectively. It is found that apodization functions is helpful to reduce the resonance attenuations of CFBGs and more importantly it can significantly suppress the side lobes.

IV. EXPERIMENTAL SETUP

A femtosecond laser grayscale lithography system was developed for the preparation of CFBGs, as illustrated in Fig. 3(a). The system employs a femtosecond laser (KY-Vibre) operating at a wavelength of 515 nm, with a pulse width of 290 fs and a repetition rate of 1000 kHz. The polarized femtosecond pulsed laser beam passes through an optical switch, an attenuator (Altechna), and a dichroic mirror before being focused by an objective lens onto the fiber core. An optical fiber is precisely positioned on a three-axis displacement platform (Aerotech ABL15010) for

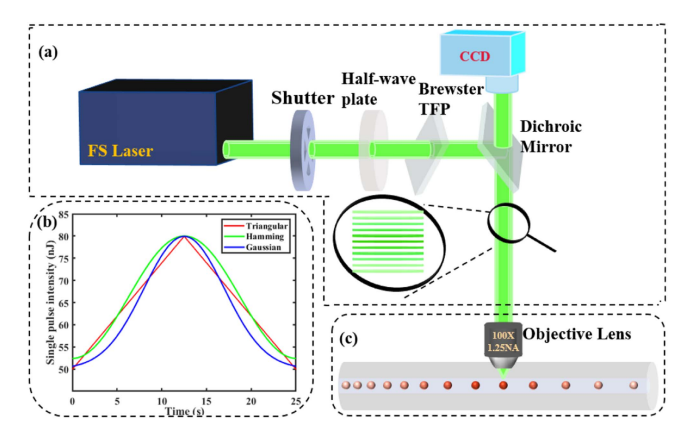


Fig. 3. The system of apodized CFBG by femtosecond laser direct writing technology: (a) the fabrication platform of apodized CFBG. FS, femtosecond; TFP, thin filmpolarizers, (b) three kinds of apodized modulation functions (i.e., Triangular, Gaussian and Hamming), and (c) the diagrammatic drawing of the apodized linear CFBG.

grating inscription. To ensure precise control throughout the fabrication process, a CCD camera is employed to provide visual feedback in real-time.

Initially, grayscale lithography system is designed to precisely control the single-pulse energy by adjusting the angle θ between the optical axis of the half-wave plate within the attenuator and the polarization direction of the Brewster film polarizer according to Malus's law:

$$I = I_0 \cos^2 \theta \tag{5}$$

Where, I represents the output optical energy, I_0 denotes the input optical energy, and θ is the angle between the optical axis of the internal half-wave plate in the attenuator and the polarization direction of the Brewster film polarizer.

A dedicated customized program is then used to regulate the functional variation of the angle θ , ensuring that the output single-pulse energy conforms to a specific apodization profile as shown in Fig. 3(b) over time. As a result, the single-pulse energy can be intentionally adjusted between 50 and 70 nJ over a time range from 0 to 25s. Consequently, the refractive index of the fiber core is modulated based on different apodization functions.

Next, to improve spectral performance and dispersion compensation, we use integrating external pulse timing control technology to fabricate apodized and highly linear CFBGs with grayscale lithography. The fabrication of linear CFBGs requires precise control over the grating period during the inscription process, which necessitates meticulous adjustment of each pulse interval. The grating period range is determined by the wavelength range of the grating. According to the Bragg grating equation:

$$\lambda(z) = \frac{2n_{eff}\Lambda(z)}{m} \tag{6}$$

Where, $\Lambda(z)$ represents a function of the grating period, m denotes the fiber order, $\lambda(z)$ is the function of the wavelength,

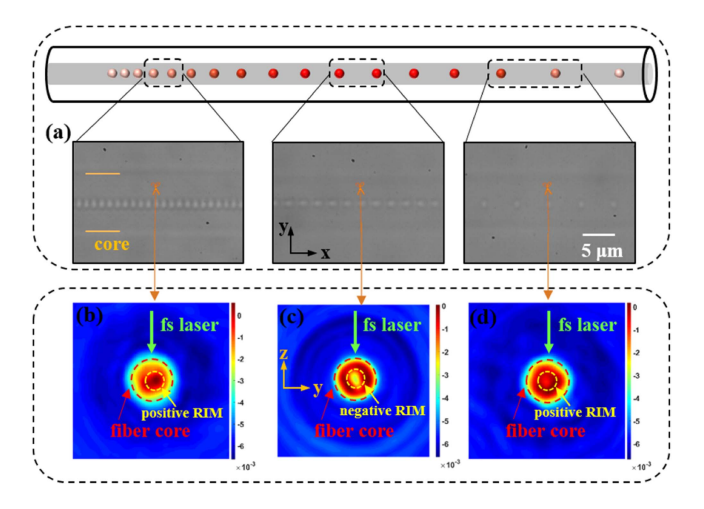


Fig. 4. Distribution and structural characterization of CFBG: (a) three parts of vertical view microscope images of CFBG, (b) refractive index distribution of the short-wavelength grating and the grating cross section in the weak energy modulation of CFBG, (c) refractive index distribution of the center wavelength grating and the grating cross section in the strong energy modulation of CFBG, and (d) refractive index distribution of the long-wavelength grating and the grating cross section in the weak energy modulation of CFBG.

and z indicates the grating position.

$$\Lambda(z) = \frac{\nu}{f_1(z)} \tag{7}$$

Where, ν corresponds to the moving speed of the three-axis displacement platform, and $f_1(z)$ represents the laser pulse output frequency function.

Therefore, the speed of the three-axis displacement platform and external pulse frequency can be derived from the target dispersion value and the chirp rate using the above equations. The external pulse timing control technique employs the calculated frequency obtained from (7) to generate a specific control signal. This signal precisely regulates the output pulse frequency of the femtosecond laser. As the laser emits pulses, the three-axis displacement platform moves synchronously, facilitating the fabrication of gratings across any desired spectral range. This method achieves a more linear delay effect, significantly enhancing both the efficiency and flexibility of the grating fabrication process.

The reflection spectra of CFBGs were measured using an OSA. A broadband laser source was input through port 1 of a circulator, and the output from port 2 was connected to the short-wavelength part of the chirped grating. The reflected light from the grating was output through port 3 and captured by the OSA. Furthermore, the transmission spectrum can be measured on the long-wavelength part of the CFBG using OSA. An optical backscatter reflectometer (OBR, Luna OBR 6400) is then used to measure the group delay of the four gratings, with a scanning range of 1535–1565 nm and a spatial resolution of 0.05 mm.

A second-order Gaussian apodized CFBG was first prepared to verify the feasibility of the developed fabrication platform. Fig. 4(a) shows the top-view microscopic images at different laser writing positions of the CFBG and the corresponding cross-sectional refractive index profiles was measured using

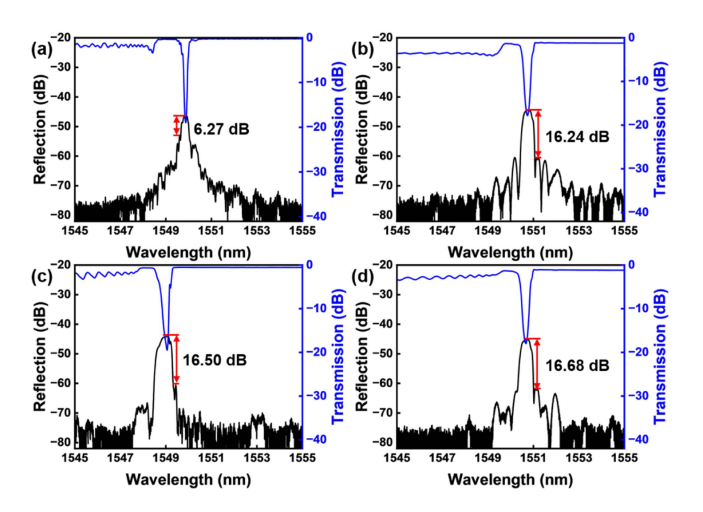


Fig. 5. Experimental reflection and transmission spectra of FBG by different apodized functions: (a) Uniform and FBG with SLSR of 6.27 dB, (b) Hamming and FBG with SLSR of 16.24 dB, (c) Triangular and FBG with SLSR of 16.50 dB, and (d) Gaussian and FBG with SLSR of 16.68 dB.

a digital holographic microscope (SHR-1602) as shown in Fig. 4(b)–(d), where the red dashed line circled area is the fiber core and the yellow dashed line circled area is the grating. It is demonstrated that both positive RIM and negative RIM can be realized by varying the input laser pulse energy. High-energy pulses introduce negative refractive index modulations at the center since they induce localized void formation within the material through nonlinear absorption, resulting in a reduction of material density. In contrast, low-energy pulses produce positive refractive index modulation results from rapid thermomechanical expansion and pressure wave propagation, leading to the formation of densified regions [30]. Therefore, the femtosecond laser gray-scale lithography fabrication system integrating with external pulse timing control technology can enable efficient and flexible fabrication of CFBGs with apodization effects and linear chirp characteristics.

V. RESULTS AND DISCUSSION

A. FBG Fabrication With Different Apodized Functions

FBGs with lengths of 5 mm and different apodization functions were fabricated and their reflection and transmission spectra are shown in Fig. 5. The resonance attenuation for gratings without apodization, and with Hamming, Triangular, and Gaussian apodization functions are -17.9 dB, -17.8 dB, -18.0 dB, and -17.9 dB, respectively. It is found that under similar resonance attenuation conditions, apodization functions can effectively suppression of side lobes, which is coincidence with simulation results as shown in Fig. 1. SLSR of gratings with different apodization function were also analyzed. The grating without apodization function exhibits a SLSR of approximately 6.27 dB (Fig. 5(a)). In contrast, the grating with a Hamming apodization function (Fig. 5(b)) achieves a significantly increased SLSR of 16.24 dB. When applying a triangular apodization function (Fig. 5(c)), the SLSR is further enhanced to 16.50 dB, while the Gaussian apodization function (Fig. 5(d)) yields the highest SLSR of 16.68 dB.

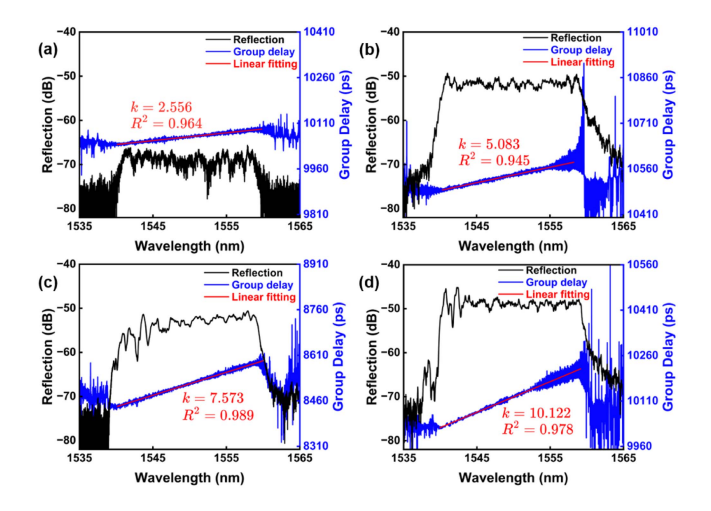


Fig. 6. The CFBG spectra of reflections and group delay with different dispersions at 20 nm bandwidths: (a) 2.5 ps/nm, (b) 5 ps/nm, (c) 7.5 ps/nm and (d) 10 ps/nm.

Compared to the reflection spectrum of the non-apodized grating, apodization gratings significantly enhance the filtering effect in the central wavelength region, which effectively improve the signal-to-noise ratio of the central reflection wavelength and yields a smoother spectral profile by suppression of side lobes. This improvement can be attributed to the self-chirping effect of FBGs, which generates prominent side lobes on both sides of the central reflection wavelength [29].

B. CFBG Fabrication Without Apodization

CFBGs without apodization is investigated to verify the reliability of the linear chirp characteristics of the fabricated CFBGs. Four chirped gratings with different amounts of dispersion were manufactured, with central wavelengths of 1550 nm and dispersion amounts of 2.5 ps/nm, 5.0 ps/nm, 7.5 ps/nm and 10.0 ps/nm, respectively. Under the same spectral bandwidth condition of 20 nm, the corresponding chirp rates for the four dispersion amounts are calculated using (4) as 39.6 nm/cm, 19.3 nm/cm, 15.5 nm/cm, and 9.6 nm/cm, respectively. The corresponding grating lengths are 5.17 cm, 10.35 cm, 15.53 cm, and 20.71 cm.

Fig. 6 displays the reflection spectra of the prepared four CFBGs and their group delay with different dispersions. According to (4), grating length is proportional to the first-order dispersion. Consequently, a shorter grating length is required for a smaller first-order dispersion and hence the grating in Fig. 6(a) exhibits weaker reflection intensity compared to the other three gratings shown in Fig. 6(b), (c) and (d). The firstorder dispersion amount can be obtained from the slope k of the fitted group delay curve within the 1540–1560 nm range. Hence the first-order dispersion amounts of the four gratings are 2.556 ps/nm, 5.083 ps/nm, 7.573 ps/nm, and 10.122 ps/nm, respectively, which are very close to the designed dispersion amounts, with errors of 0.056 ps/nm, 0.083 ps/nm, 0.073 ps/nm, and 0.122 ps/nm, respectively. The errors were maintained within 0.2 ps/nm, demonstrating the high reliability of the fabricated linearly CFBGs. In the experiment, lower group delay ripples were observed at a shorter wavelength as illustrated in

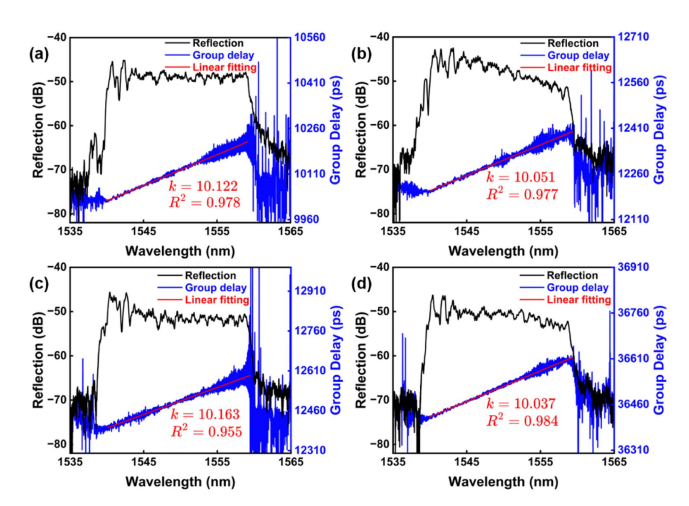


Fig. 7. The spectra of reflections and group delay of CFBG after different apodized functions (a) not apodized function; (b) Hamming function; (c) Triangular function; (d) Gaussian function.

Fig. 6(a)–(d). This phenomenon can be attributed to the increased grating period configuration of the chirped fiber grating, where a shorter wavelength is reflected earlier than a longer wavelength, and hence a longer wavelength experiences a higher insertion loss due to longer propagation path, leading to poorer linearity in the group delay curves.

C. CFBG Fabrication With Apodization

To mitigate the ripple effect in the group delay curve, apodization functions were introduced into the CFBGs, and their effects on the group delay characteristics were investigated and the corresponding reflection spectra are shown in Fig. 7. The grating parameters was preset as: a first-order dispersion of 10 ps/nm, a grating length of 20.71 mm, a bandwidth of 20 nm, a central wavelength of 1550 nm, and a chirp rate of 9.66 nm/cm. As can be seen from Fig. 7, the first-order dispersion errors for not apodized function, Hamming, Triangular, and Gaussian apodized CFBGs were 0.122 ps/nm, 0.051 ps/nm, 0.163 ps/nm, and 0.037 ps/nm, respectively, with error controlled within 0.2 ps/nm. Additionally, the corresponding R² (linear fitting coefficient) are 0.978, 0.977, 0.955, and 0.984, respectively. A larger R² value indicates a better fit of the group delay slope curve and reduced oscillations in the group delay curve. Hence it is demonstrated that the Gaussian apodization function improves the CFBGs' reflection spectrum by achieving a SLSR exceeding 15 dB while simultaneously enhancing the linearly of the group delay.

VI. CONCLUSION

In conclusion, a grayscale lithography and external pulse timing control technique are proposed for fabrication of apodized FBGs and apodized CFBGs, systematically investigation on the impact of apodization functions on the side-lobe suppression ratio and group delay characteristics are conducted. Both simulation and experimental results confirm that the Gaussian apodization function delivers superior performance in side-lobe suppression (>15 dB), signal-to-noise ratio (>10 dB), and

overall spectral response. Notably, this function mitigate group delay oscillations induced by linear CFBGs [31]. Furthermore, by employing external pulse timing control techniques, CFBGs with dispersion errors below 0.2 ps/nm can be fabricated, further enhancing the linearity of group delay. Leveraging this efficient grating fabrication system, it is possible to customize the preparation of linearly CFBGs according to diverse dispersion compensation requirements and arbitrary apodization functions, which offers new possibilities for not only enhancing the performance of devices such as filters, fiber lasers, and dispersion compensators but also opens up novel technical pathways for fiber grating fabrication and applications.

REFERENCES

- C. Ghosh and V. Priye, "Dispersion compensation in a 2420 Gbps DWDM system by cascaded chirped FBGs," Optik, vol. 164, pp. 335–344, 2018.
- [2] G.R. Sreeragi, N. Vijayakumar, and R. Pradeep, "A novel approach integrating CFBG and optical filters to mitigate CD and PMD effects in high speed DWDM fiber optic links," *Opt. Quantum Electron.*, vol. 56, no. 8, 2024, Art. no. 1283.
- [3] Z. Cai et al., "Encrypted optical fiber tag based on encoded fiber bragg grating array," Int. J. Extreme Manuf., vol. 5, no. 3, 2023, Art. no. 035502.
- [4] A. Dmitriev, S. Varzhel, K. Grebnev, and E. Anokhina, "Strain gauge based on n-pairs of chirped fiber Bragg gratings," *Opt. Fiber Technol.*, vol. 70, 2022, Art. no. 102893.
- [5] Y. Lu, C. Baker, L. Chen, and X. Bao, "Group-delay-based temperature sensing in linearly-chirped fiber Bragg gratings using a Kerr phase-interrogator," *J. Lightw. Technol.*, vol. 33, no. 2, pp. 381–385, Jan. 2015.
- [6] C. Liao et al., "Design and realization of 3D printed fiber-tip microcantilever probes applied to hydrogen sensing," *Light: Adv. Manuf.*, vol. 3, no. 1, pp. 3–13, 2022.
- [7] K. Li et al., "Long chirped fiber grating pressure tactile sensing," *Opt. Fiber Technol.*, vol. 72, 2022, Art. no. 102939.
- [8] M. Zou et al., "3D printed fiber-optic nanomechanical bioprobe," *Int. J. Extreme Manuf.*, vol. 5, no. 1, 2023, Art. no. 015005.
- [9] V. Remesh et al., "Compact chirped fiber Bragg gratings for single-photon generation from quantum dots," APL Photon., vol. 8, no. 10, 2023, Art. no. 101301.
- [10] T. Bartulevicius et al., "Compact femtosecond 10 μ J pulse energy fiber laser with a CFBG stretcher and CVBG compressor," *Opt. Fiber Technol.*, vol. 45, pp. 77–80, 2018.
- [11] F. Li et al., "Hybrid fiber-single crystal fiber chirped-pulse amplification system emitting more than 1.5 GW peak power with beam quality better than 1.3," *J. Lightw. Technol.*, vol. 42, no. 1, pp. 381–385, Ian 2024
- [12] M. Becker, T. Elsmann, I. Latka, M. Rothhardt, and H. Bartelt, "Chirped phase mask interferometer for fiber Bragg grating array inscription," *J. Lightw. Technol.*, vol. 33, no. 10, pp. 2093–2098, May 2015.

- [13] C. Voigtländer et al., "Chirped fiber Bragg gratings written with ultrashort pulses and a tunable phase mask," Opt. Lett., vol. 34, no. 12, pp. 1888–1890, 2009.
- [14] S. Wang et al., "High reflectivity, ultraflat-spectrum chirped fiber bragg grating written using low energy UV femtosecond pulses," Opt. Laser Technol., vol. 176, 2024, Art. no. 111035.
- [15] S. R. Baker, H. N. Rourke, V. Baker, and D. Goodchild, "Thermal decay of fiber Bragg gratings written in boron and germanium codoped silica fiber," *J. Lightw. Technol.*, vol. 15, no. 8, pp. 1470–1477, Aug. 1997.
- [16] C. Zhang, Y. Yang, C. Wang, C. Liao, and Y. Wang, "Femtosecond-laser-inscribed sampled fiber bragg grating with ultrahigh thermal stability," *Opt. Exp.*, vol. 24, no. 4, pp. 3981–3988, 2016.
- [17] M. Y. Koptev et al., "Chirped fiber bragg gratings directly inscribed by a femtosecond laser in an ytterbium-doped fiber for spectrum recovery, loss compensation and effective use in a CPA scheme," Opt. Laser Technol., vol. 181, 2025, Art. no. 111989.
- [18] P. Lu et al., "Plane-by-plane inscription of grating structures in optical fibers," *J. Lightw. Technol.*, vol. 36, no. 4, pp. 926–931, Feb. 2018.
- [19] X. Xu et al., "Slit beam shaping for femtosecond laser point-by-point inscription of high-quality fiber Bragg gratings," *J. Lightw. Technol.*, vol. 39, no. 15, pp. 5142–5148, Aug. 2021.
- [20] K. Hinton, "Dispersion compensation using apodized bragg fiber gratings in transmission," *J. Lightw. Technol.*, vol. 16, no. 12, pp. 2336–2346, Dec. 1998.
- [21] R. J. Williams et al., "Point-by-point inscription of apodized fiber bragg gratings," Opt. Lett., vol. 36, no. 15, pp. 2988–2990, 2011.
- [22] S. Antipov et al., "Direct infrared femtosecond laser inscription of chirped fiber Bragg gratings," Opt. Exp., vol. 24, no. 1, pp. 30–40, 2016.
- [23] H. Zheng et al., "Large-scale metasurfaces based on grayscale nanosphere lithography," *ACS Photon.*, vol. 8, no. 6, pp. 1824–1831, 2021.
- [24] Z. Ding, H. Wang, T. Li, X. Ouyang, Y. Shi, and A. P. Zhang, "Fabrication of polymer optical waveguides by digital ultraviolet lithography," *J. Lightw. Technol.*, vol. 40, no. 1, pp. 163–169, Jan. 2022.
- [25] Z. Gan et al., "Spatial modulation of nanopattern dimensions by combining interference lithography and grayscale-patterned secondary exposure," *Light: Sci. Appl.*, vol. 11, no. 1, 2022, Art. no. 89.
- [26] R. Mingesz et al., "Enhanced control of excimer laser pulse timing using tunable additive noise," *Fluctuation Noise Lett.*, vol. 11, no. 01, 2012, Art. no. 1240007.
- [27] T. Erdogan, "Fiber grating spectra," J. Lightw. Technol., vol. 15, no. 8, pp. 1277–1294, Aug. 1997.
- [28] D. Tan, X. Sun, and J. Qiu, "Femtosecond laser writing low-loss waveguides in silica glass: Highly symmetrical mode field and mechanism of refractive index change," *Opt. Mater. Exp.*, vol. 11, no. 3, pp. 848–857, 2021.
- [29] D. Pastor, J. Capmany, D. Ortega, D. Ortega, V. Tatay, and J. Marti, "Design of apodized linearly chirped fiber gratings for dispersion compensation," *J. Lightw. Technol.*, vol. 14, no. 11, pp. 2581–2588, Nov. 1996.
- [30] L. Matulic and J. H. Eberly, "Analytic study of pulse chirping in selfinduced transparency," *Phys. Rev. A*, vol. 6, no. 2, 1972, Art. no. 822.
- [31] M. Sumetsky, B. J. Eggleton, and C. M. de Sterke, "Theory of group delay ripple generated by chirped fiber gratings," *Opt. Exp.*, vol. 10, no. 7, pp. 332–340, 2002.